DTU Library

Particle Distribution in a Fixed Bed Down Draft Wood Gasifier

Hindsgaul, Claus

Published in:
Proceedings of 14th European Conference and Exhibition: Biomass for Energy, Industry and Climate Protection

Publication date:
2005

Document Version
Publisher's PDF, also known as Version of record

PARTICLE DISTRIBUTION IN A FIXED BED DOWN DRAFT WOOD GASIFIER

Claus Hindsgaul and Ulrik Henriksen
Department of Mechanical Engineering, Technical University of Denmark (DTU)

ABSTRACT:
Char particle samples were collected from six distances above the grate in a fixed bed of a down draft biomass gasifier. Each sample was separated into twelve size fractions by screening through standard sieves in order to determine the local particle size distribution. The ash contents of each particle fraction was determined. The measured ash content in the larger particles was nearly constant throughout the bed, while ash accumulated in particle sizes around 1 mm near the bottom.
Keywords: downdraft gasifier, fixed bed, wood char

1 INTRODUCTION

Knowledge on the processes inside fixed bed gasifiers is required to build and validate detailed computer models of the process. This work investigates the fate of particles undergoing thermal conversion in a fixed gasification bed by mapping the particles sizes and ash content at different distances above the grate in a fixed bed down draft gasifier. The results quantify the change in particle sizes during conversion and the distribution of the ash.

2 THEORY

In a fixed bed down draft gasifier, the carbon in the particles in the bed reacts chemically with O_2 and H_2O in the gas flowing through the bed. Thus the carbon content in particles is decreasing from the top to the supporting grid at the bottom. The size distribution of the particles is expected to shift toward smaller particles due to lost carbon at their surface and disintegration due to increasing structural weaknesses in the particles and increased mechanical stress from the bed above. An opposite effect happens as the smallest particles escape with the gas.

The sample mass, M, and the (randomly packed) volume, V, can be easily measured for a given sample of char. The sample density is then:

$$\rho = \frac{M}{V}$$

After completely oxidizing the sample, the mass of the ash present in the sample, M_{ash}, can be found. The ash mass fraction, m_{ash}, and the ash density, ρ_{ash}, (the amount of ash per volume in the original sample) is then:

$$m_{ash} = \frac{M_{ash}}{M}$$

$$\rho_{ash} = m_{ash} \cdot \rho$$

A particle sample can separated into discrete size ranges by screening the sample through standard sieves. In the following, properties for a given size range will be marked with subscript s. By determining the mass M_s of every size range, the mass fraction of particles within each size range, m_s, can be obtained by:

$$m_s = \frac{M_s}{M} = \frac{M_s}{\sum_{s=1}^{NS} M_s}$$

Where M is the total sample mass and NS is the total number of size ranges. After complete oxidation of particles from a size range, the ash fraction in this size range, $M_{ash,s,}$ can be measured. The ash mass fraction in this size range is:

$$m_{ash,s} = \frac{M_{ash,s}}{M_s}$$

The ash fraction of the total sample can be found by summarising the individual size fractions:

$$m_{ash} = \frac{M_{ash}}{M} = \frac{\sum_{s=1}^{NS} M_{ash,s}}{\sum_{s=1}^{NS} M}$$

The mass of a particle size range per volume sample will be called the particle range density ρ_s:

$$\rho_s = \frac{M_s}{V} = \rho \cdot m_s$$

The mass of ash per volume sample, $\rho_{ash,s}$:

$$\rho_{ash,s} = \frac{M_{ash,s}}{V} = \rho \cdot m_s \cdot x_s$$

Note that all densities in this paper will be based on some mass divided by the randomly packed volume of the *original* sample containing all particle size ranges.

3 EXPERIMENTAL

3.1 The char samples

The investigated char samples were taken from the remaining bed after an experiment of a down draft biomass gasifier fuelled by wood chips. The gasifier was the 100 kW two stage gasifier at DTU (Bentzen et al., 1999), which is the same type as the Viking gasifier (Gøbel et al. 2004). It is an air blown down draft two stage gasifier (with a separate pyrolysis reactor). The test was done in January 1998 and lasted 72 hours. Temperatures in the bed ranged from approximately 800 ˚C near the top to 680 ˚C at the grate. When the test was finished, N_2 was led into the reactor to stop all reactions until the bed had cooled down.

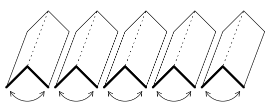

Figure 1: The grate supporting the coke bed during gasification.

The grate, which supported the char bed consisted of V-shaped metal sticks which — when rotated — could increase the width of the openings between them. See Figure 1. The char was removed from the reactor by gently tilting these sticks. As the material near the grate was removed, its original position in the bed was estimated by measuring the distance from the top of the reactor to the top of the bed.

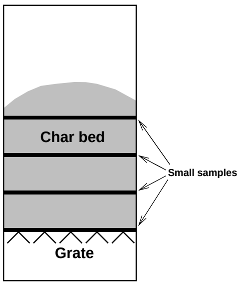

Figure 2: Original locations of samples in the bed of the fixed bed gasifier. Each "small sample" was divided into 12 size ranges by screening.

Samples from different positions in the bed were collected in separate containers labelled by its estimated original distance above the supporting bed. The top of the bed was 145 cm above the grate. Small samples (120--170 g) were collected through the grate from original distances 0, 17, 59, 79, 101 and 121 cm above the grate. Between these samples, large bags with several kg material were collected. All mass determinations of the investigated char samples were done after drying at 104 ˚C.

3.2 Sample densities

The bulk volume of each screened sample was measured before screening, and the bulk density of the sample calculated. For comparison, approximate bed densities were also calculated from data collected while the char bed was emptied: the removed mass and the corresponding vertical movement of the top of the bed. The resulting densities are shown in Figure 3. While both methods give densities between 50 and 140 kg/m^3, they show no consistent trend The direct measurements ("sample") were considered to be the most accurate, and will be used in the calculations..

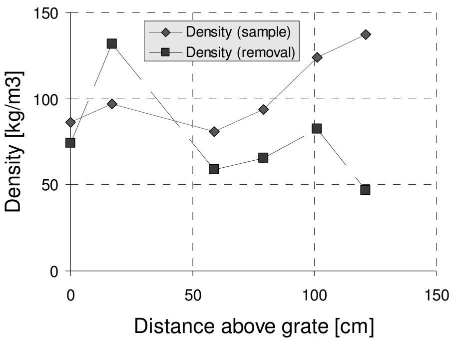

Figure 3: Density ρ of bulk particles at different distances above the grate calculated from observations while removing the coke from the bed (removal) and measurements on the samples (sample).

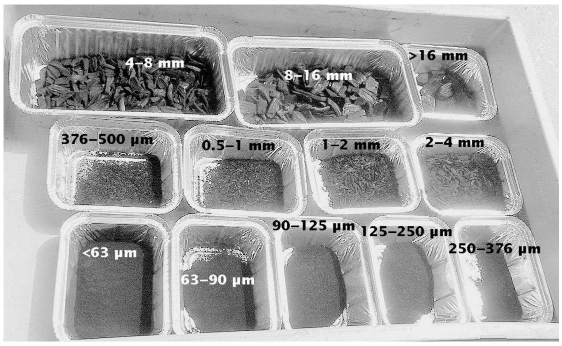

Figure 4: Screened sample.

3.3 Screening

The screening was done using 11 standard Endecotts Sieves with grid sizes ranging from 63 µm to 16 mm. The sieves were mounted in a sieve shaker and the particle samples were shaken for 40 minutes. Test screenings showed, that the amount of particles, which reached the bottom had stabilized after this amount of time. Figure 4 shows the screened particles from one sample.

After the screening, the particle sample was dried at 104 ˚C for 16 hours before their masses, m_s, were determined. The cumulated size distributions for all the bed samples are shown in Figure 5. In order to evaluate particle breakage during screening a batch of big char lumps (>8 mm) where hand picked and screened. The resulting size distribution ("Big lumps" in Figure 5) shows that 4% of the lumps ended up in the smallest particle fraction. Another 3% appear between 63-500 µm, while insignificant amounts are found between 0.5-8 mm. These particles have two sources: char dust stuck to the surface of the collected lumps and small fragments generated during screening. Note that apparently neither of these sources any significant amount of particles in the 0.5-8 mm range.

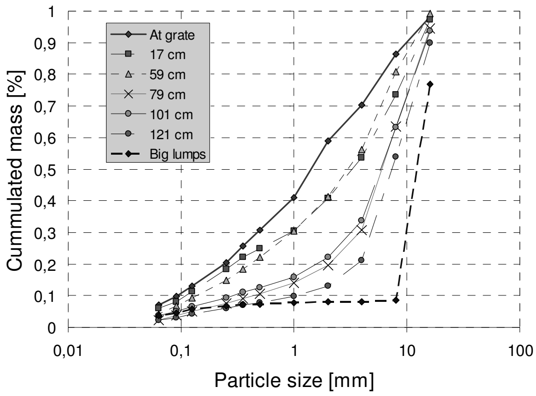

Figure 5: Cumulated particle size distribution of screened samples.

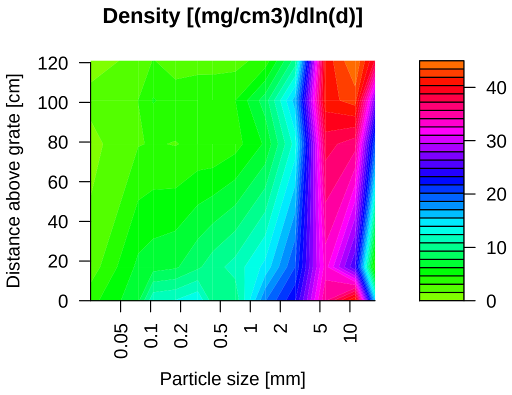

Figure 6: Mass of particles of the given sizes per volume bed material, ρ_s.

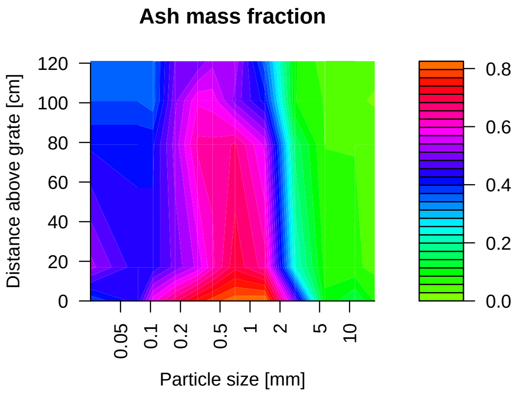

Figure 7: Contour plot of $m_{ash,s}$ (data from Table I).

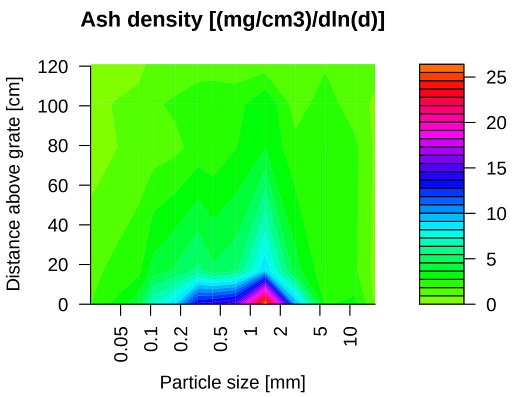

Figure 8: Mass of ash contained in particles of the given sizes per volume bed material, $\rho_{ash,s}$.

As expected, the size distribution shifts towards smaller particles as the char travels down through the bed. But since the total density ρ of the bed increase towards the bottom, it turns out that the mass of large particles per bed volume, (ρ_s for large particles) does not change as much as the particle size distribution would suggest. Figure 6 shows a contour plot of the particle size range densities, ρ_s. In order to achieve a continuous representation, the contour values in this graph (and similar graphs throughout this paper) were divided by the difference of the logarithms of the largest and the smallest particle diameter in the range. It is clear from this graph, that the mass of particles >5 mm per volume bed is nearly constant, while the mass of particles with sizes 0.2-5 mm per bed volume increase rapidly near the grate.

Particle size	121cm	101cm	79cm	17cm	0cm
>16 mm	3,3%	2,7%	3,8%	5,0%	8,1%
8-16 mm	3,6%	3,1%	5,6%	6,2%	14,4%
4-8 mm	4,2%	5,5%	5,6%	7,8%	9,0%
2-4 mm	9,0%	8,7%	16,1%	23,1%	49,7%
1-2 mm	35,3%	41,4%	56,1%	64,0%	82,5%
0,5-1 mm	53,2%	50,2%	65,9%	70,3%	81,4%
355-500 µm	53,2%	58,5%	63,4%	62,0%	78,4%
250-355 µm	48,6%	59,3%	63,4%	54,9%	75,3%
125-250 µm	48,6%	50,5%	52,5%	49,4%	67,6%
90-125 µm	35,7%	35,3%	42,2%	43,6%	58,7%
63-90 µm	35,7%	36,9%	42,2%	43,6%	44,0%
0-63 µm	35,7%	36,9%	42,2%	52,2%	37,5%
Weighed average	9,3%	13,7%	16,4%	29,4%	37,5%

Table I: Ash mass fractions in individual samples ($m_{ash,s}$). The boxes mark samples which were mixed before ash determination due to low individual masses (<2 g).

3.4 Ash content

The ash content of each particle size fractions, $M_{ash,s}$, from samples taken 0, 17, 79, 101 and 121 cm above the grate were determined by measuring the residual mass after heating the sample to 550 ˚C in the presence of O_2 for several hours. Table I shows the derived ash mass fractions, $M_{ash,s}$, in the different particle size ranges at the different distances above the grate, while Figure 7 shows a contour plot of the same data.

Particles around 1 mm generally have a higher ash content than other size ranges. This effect become increasingly significant as the grate is approached. Also, the ash content of the larger particles is relatively constant.

Figure 8 shows the ash mass for different particle sizes per bed volume, ρ_s. Due to the relatively high density of particles around 1 mm and the high ash content of this particle size, the ash density for this particular particle size become very high near the grate compared to any other particle. The highest measured value of $\rho_s/\text{dln}(d)$ was 26.4 mg/(cm^3·ln(mm)) found in the particle size range 1-2 mm at the grate.

In order to quantify how the carbon of a batch of char added to the top of the bed is depleted on its way through the bed, is assumed that the ash does not leave the particles (e.g. by evaporation) and that particles of different sizes travel through the bed together. It is likely that a fair amount of smaller particles may travel through the bed, so this assumption may be a bit rough. Under these assumptions, observe a control volume at the top of the fixed bed defined by a fixed amount of ash and the carbon contained in the same char particles. The carbon M_{carbon} decrease due to gasification as these char particles move downwards with the bed, while the ash mass M_{ash} is constant. Thus the mass of the sample will be

$$M_{ash} = M \cdot m_{ash} = M^0 \cdot m^0_{ash}$$

$$\Leftrightarrow M^0 = \frac{m_{ash}}{m^0_{ash}} \cdot M$$

For a particle size range, the carbon mass relative to the *original* total mass, M^0 is:

$$\frac{M_{carbon,s}}{M^0} = \frac{M_{carbon,s}}{M} \cdot \frac{m^0_{ash}}{m_{ash}} = (M - M_{ash,s}) \cdot \frac{m^0_{ash}}{m_{ash}}$$

Figure 9 shows a plot of this ratio. It shows how the residual carbon mass is present but decays in the largest particles. The corresponding plot for the distribution of the ash content mass relative to the original total mass is shown in Figure 10. The migration of ash to particles around 1 mm is also clear in this plot.

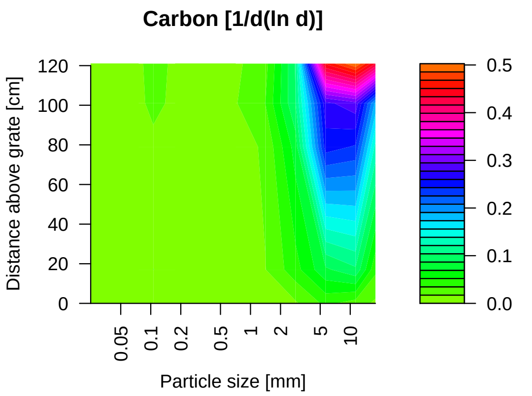

Figure 9: Carbon mass in the given particle size fractions relative to the total mass of the same char control volume at the top of the fixed bed, $\frac{M_{carbon,s}}{M^0}$.

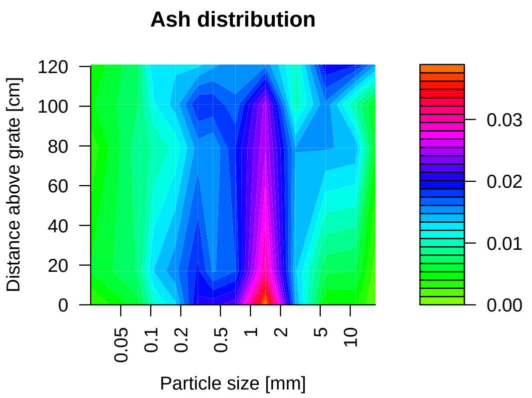

Figure 10: Ash mass in the given particle size fractions relative to the total mass of the same char control volume at the top of the fixed bed, $\frac{M_{ash,s}}{M^0}$.

4 CONCLUSIONS

The particle size distribution and ash content in different particle sizes were determined in the bed of a down draft fixed bed gasifier.

Near the bottom of the bed, char particles around 1 mm contained much more ash (80%) than the larger ones (<10%). This indicate that char particles >4 mm in the bottom ash can be returned to the reactor for further gasification.

The ash tends to end up in a narrow particle size around 1 mm. This may be partly caused by the method used to divide the sample into size fractions, since sieving may have removed a layer of a high degree of conversion from the larger particles by abrasion. To a certain extend such abrasion can be expected to occur bed too. A test screening of hand picked larges char particles did not produce any significant amount of particles between 0.5-4 mm, but 7% of the mass ended as particle fractions below 0.5 mm. Thus abrasive fragmentation during screening was not likely to be responsible for the ash rich particles around 1 mm observed.

The highly uneven distribution of ash between particle sizes means that it is extremely important to collect a representative size distribution when collecting a sample from a larger batch of bottom ash for determination of the average ash content and degree of conversion. Otherwise the result may be very far from the true value.

AKNOWLEDGEMENTS

This work was financed by the Danish Energy Agency.

LITERATURE

Bentzen, J. D., Brandt, P., Gøbel, B., Hansen, C. H., and Henriksen, U. (1999). *Optimering af 100 kw totrinsforgasningsanlæg på DTU*. Technical report, DTU.

Gøbel, B, Henriksen, U., Ahrenfeldt, J., Jensen, T. K., Hindsgaul, C., Bentzen, J. D., Sørensen, L. H. (2004). *Status - 2000 Hours of Operation with the Viking Gasifier*. OE1.5 in proceedings of 2nd World Conference and Technology Exhibition on Biomass for Energy and Industry, Rom. June 2004.